IIETA International Information and Engineering Technology Association
Advancing the World of Information and Engineering

Journal Européen des Systèmes Automatisés
Vol. 58, No. 5, May, 2025, pp. 1017-1030
Journal homepage: http://iieta.org/journals/jesa

Impact of Hydrogen-Enriched CNG on Combustion Phasing, Fuel Efficiency, and Emissions in a Multi-Cylinder Spark-Ignition Engine under Varying Loads

Prasanna Sutar[1,2], Ravi Sekhar[1*], Sukrut Thipse[2], Sandeep Rairikar[2], Shailesh Sonawane[2], Debjyoti Bandyopadhyay[2], Ajinkya Jadhav[3]

[1] Symbiosis Institute of Technology (SIT), Pune Campus, Symbiosis International (Deemed University), Pune 412115, India
[2] Automotive Research Association of India (ARAI), Pune 411038, India
[3] Department of Mechanical Engineering, Jacobs School of Engineering, University of California, San Diego CA 92093, United States

Corresponding Author Email: ravi.sekhar@sitpune.edu.in

https://doi.org/10.18280/jesa.580515

Received: 31 March 2025
Revised: 5 May 2025
Accepted: 17 May 2025
Available online: 31 May 2025

Keywords:
Hydrogen-Enriched CNG (HCNG), combustion phasing, Heat Release Rate (HRR), emission characteristics, alternative fuels

ABSTRACT

The present study considered the combustion, performance and emission characteristics of a spark-ignition engine running different blends of Hydrogen-Enriched Compressed Natural Gas (HCNG) at stepwise Brake Mean Effective Pressure (BMEP). Experimental testing was completed using base Compressed Natural Gas (CNG) and HCNG blends with hydrogen by volume percentages of 18%, 25% and 30% (vol%). The combustion study showed that, in general, the higher hydrogen fractions increased the Rate of Pressure Rise (RoPR), cumulative Heat Release Rate (HRR), and in-cylinder temperature, particularly under low load conditions. Improvements were seen in combustion phasing with decreased durations for Mass Burned Fraction at 50% (MBF50%) and improved temperature gradients. The improvements in combustion characteristics translated into better engine performance with reduced Brake Specific Fuel Consumption (BSFC) at all operating loads, especially at BMEP 1.5 bar. A reduction in Carbon Monoxide (CO) and hydrocarbons (HC) was noted with the increase in hydrogen volume percentage. The NO_x emissions produced exhibited non-linear behaviour attributed to the influence of a higher flame temperature and excess air ratio. The results verified the additive benefits of HCNG on engine efficiency and emissions reduction, confirming the fuel source as a sustainable alternative fuel for next-generation spark-ignition engines.

1. INTRODUCTION

1.1 Background and motivation for alternative gaseous fuels

The transportation sector accounts for a significant portion of Global Greenhouse Gas (GHG) emissions, prompting the urgent need to transition toward cleaner and more sustainable fuels. Among various alternatives, gaseous fuels have attracted particular attention due to their inherently lower carbon content, reduced particulate emissions, and compatibility with existing internal combustion engine architectures. Compressed Natural Gas (CNG) has emerged as a strong candidate due to its widespread availability, economic viability, and relatively clean combustion profile [1]. However, as decarbonization efforts intensify, researchers are increasingly investigating hydrogen-enriched fuel mixtures to push combustion efficiency and emission reduction to new frontiers [2].

1.2 Challenges with CNG-Only engines

Despite its environmental and economic appeal, CNG presents several limitations when used as the sole fuel in spark-ignition (SI) engines. Key challenges can be lower flame propagation speed, higher auto-ignition temperature, and limited lean-burn capability restrict the engine performance and increase the risk of misfire under low-load or lean conditions. Apart from that, the slower combustion of CNG leads to increased combustion duration and suboptimal thermal efficiency, which negatively affects engine performance [3]. Furthermore, emissions of undesirable gases such as unburned methane (CH_4), Carbon Monoxide (CO), and Formaldehyde (HCHO) in the exhaust can directly impact ambient air quality and harm the environment [4]. These issues hinder CNG's potential to fully displace conventional fuels in high-performance or high-efficiency applications.

1.3 Advantages of hydrogen enrichment in SI engines

Blending hydrogen with CNG—forming Hydrogen-Enriched Compressed Natural Gas (HCNG)—offers a technically feasible approach to mitigate the aforementioned limitations. Hydrogen's high flame speed, broad flammability range, and low ignition energy facilitate more rapid and stable combustion, especially under lean and low-load conditions [5].

HCNG blends have been shown to improve in-cylinder pressure profiles, reduce ignition delay, and increase the rate of heat release (HRR), contributing to improved brake thermal efficiency and reduced hydrocarbon (HC) and CO emissions [6]. However, one trade-off is a potential rise in NO_x emissions due to increased peak combustion temperatures, necessitating careful blend optimization and emissions after-treatment strategies [7].

1.4 Literature review summary

A growing body of experimental and computational research supports the use of HCNG in SI engines. Kalsi Subramanian [8] investigated the effect of varying hydrogen concentration in CNG blends and observed that 30% HCNG yielded the most significant improvements in combustion efficiency and engine output. Similarly, Mustafi and Agarwal [9], reported that HCNG enables reliable lean combustion even under part-load conditions, a key limitation in pure CNG engines. A comparative assessment by Luo et al. [10] underscored the trade-off between improved combustion and NO_x emissions in HCNG-fueled engines. Their study noted that higher hydrogen ratios accelerate MBF50 and shorten combustion duration but require careful spark timing optimization to prevent knocking. Khab et al. [11], performed real-time experiments on HCNG dual-fuel configurations and found that increased hydrogen ratios enhanced HRR but necessitated upgraded ignition and cooling systems. Prasad and Agarwal [12] compared spark and laser ignition methods using HCNG blends and found that hydrogen enrichment led to better stability, higher peak pressures, and improved MBF50 characteristics. Despite these advantages, studies emphasized the importance of analyzing performance under real-world load variations to establish optimal blend ratios and engine tuning strategies.

Notwithstanding these significant contributions, the majority of the extant literature is constrained to investigations involving single-cylinder or constant-load scenarios, which fail to encapsulate the intricacies associated with real-world driving dynamics or the variable load fluctuations characteristic of commercial applications. Furthermore, there exists a paucity of comparative data regarding the performance of HCNG blends with varying hydrogen fractions within the same engine framework across a diverse array of operational conditions.

1.5 Objectives and novelty of the current study

This research endeavours to bridge the prevailing gaps in the literature by executing a comprehensive experimental analysis of HCNG blends—specifically 18%, 25%, and 30% hydrogen by volume—utilizing a naturally aspirated, 6.5-liter multi-cylinder SI engine. In contrast to the majority of previous investigations, the present study emphasizes the combustion characteristics and engine performance under single-speed operation across various load conditions, thereby closely simulating real-world applications. Fundamental combustion parameters, such as in-cylinder pressure, mean combustion phasing or 50% Mass Burnt Fraction (MBF50), HRR, duration of combustion, and exhaust temperature, are examined in conjunction with engine performance indicators, including Brake Mean Effective Pressure (BMEP) and Brake-Specific Fuel Consumption (BSFC). The findings are intended to elucidate the impact of varying hydrogen concentrations on combustion phasing, efficiency, and stability within a multi-cylinder engine configuration.

The originality of this study is fundamentally rooted in its emphasis on operational realism and blend-level granularity. Through a methodical comparison of various HCNG concentrations subjected to controlled yet fluctuating engine loads, this investigation yields essential insights regarding the optimal level of hydrogen substitution that achieves an equilibrium between combustion efficiency, emission control, and mechanical integrity. The findings possess immediate relevance for the advancement of HCNG-based propulsion technologies as interim solutions in the pursuit of carbon-neutral mobility.

2. EXPERIMENTAL SETUP

2.1 Engine specifications

The experimental investigation was conducted using a 6.5-liter, naturally aspirated, water-cooled, four-stroke, multi-cylinder SI engine. The engine features a total displacement of 6.5 liters. It is equipped with an electronically adjusting mixer system, conventional spark plug ignition and is designed to operate on gaseous fuels. The compression ratio was maintained at 17.1:1 to ensure compatibility with both pure CNG and HCNG blends without inducing knocking. A high-energy ignition coil and an advanced ignition timing controller were employed to provide precise spark timing, particularly critical for higher hydrogen content blends due to their lower ignition energy and faster combustion characteristics. The engine specifications are given in Table 1.

Table 1. Engine specifications

No. of Cylinders	06 - Inline
Engine Displacement	6.50 liter
Aspiration	Naturally Aspirated
Rated Speed	1500 RPM
Max. Power	85 HP
Ignition System	Electronic spark ignition
Fuel System	Electronically adjusting gas-air mixer
Ignition System	Electronic-assisted spark ignition

The engine was mounted on a heavy-duty testbed and coupled with an eddy current dynamometer to allow for precise control of speed and load conditions during the tests. The engine's performance and combustion metrics were monitored in real-time using a centralized control system integrated with advanced instrumentation.

2.2 Fuel blends

Four fuel configurations were evaluated:

- **CNG (0% hydrogen)** – Serving as the baseline fuel, composed primarily of methane (~95% CH_4), with small amounts of Ethane, Nitrogen, and Carbon Dioxide. The detailed CNG composition is given in Table 2.
- **18HCNG** – A blend containing 18% hydrogen by volume and 82% CNG.
- **25HCNG** – A mid-range blend with 25% hydrogen.
- **30HCNG** – The highest hydrogen content tested in this study, composed of 30% H_2 and 70% CNG.

The blends were prepared using precision gas mixing units equipped with mass flow controllers, ensuring consistent

volumetric ratios. The gases were stored in ISO 9809-compliant high-pressure cylinders, filtered for moisture and particulates, and validated using gas chromatography, as per standard HCNG blending practices.

Table 2. Detailed CNG composition

Sr. No.	Composition	Gas Composition (Mole%)
1.	Hexane (C6+)	0.06418
2.	Nitrogen (N2)	0.23291
3.	Methane (C1)	95.12038
4.	Carbon dioxide (CO_2)	1.16103
5.	Ethane (C2)	2.16364
6.	Propane (C3)	0.83894
7.	I - Butane (IC4)	0.13691
8.	N - Butane (NC4)	0.19643
9.	I - Pentane (IC5)	0.04533
10.	N - Pentane (NC5)	0.04026
11.	Total	100.00

2.3 Engine dynamometer and data acquisition systems

The engine was coupled to a 150kW eddy current dynamometer equipped with a load cell for torque measurement and a high-precision shaft encoder for crank angle resolution (up to 0.1° CA). The dynamometer was controlled through a programmable electronic controller in the test cell Automation system, capable of maintaining constant engine speed and varying engine load with high repeatability. The schematic engine test setup is shown in Figure 1.

An AVL GH15D piezoelectric pressure transducer was installed in one cylinder to measure real-time in-cylinder pressure data. The sensor was linked to an AVL FI Piezo charge amplifier, which transmitted signals to a high-speed data acquisition system (HSDA System), AVL Indimicro. Pressure signals were logged over 300 consecutive engine cycles at each operating condition to account for cycle-to-cycle variation. The start of combustion and heat release analysis were determined using the first derivative of pressure with respect to crank angle and applying the Rassweiler-Withrow method for HRR calculations. The complete instrumentation is given in Table 3.

In addition to pressure data, thermocouples (K-type) were installed at key locations, including the exhaust manifold and intake plenum, to measure gas temperatures. Exhaust gas emissions were not the focus of this paper, but were recorded using an AVL AMAi60 raw gas analyser to ensure combustion completeness and safety monitoring.

Table 3. Instrumentation for test data acquisition

Equipment	Make
Engine Steady State Dynamometer	SAJ, AG-150
Test Cell Automation System	iASYS, ORBIT-e
Air Handling Conditioned Unit	KS_ENG_IACU3000
Raw Emission Analyzer	AVL AMA i60-01
Air Flow Meter	ABB Sensyflow, SFI
Gas Flow Meter	Krohne-Marshall CFM 01
Combustion Data Acquisition System	AVL Indi Micro

2.4 Test conditions: Single-speed operation with varying load levels

The engine was operated at a constant speed of 1500 RPM. For each fuel blend, the engine was subjected to four load levels represented by BMEP as 1.5 bar, 3.7 bar, 6 bar and 7.5 bar, to assess the impact of engine loading on combustion performance and stability.

At each operating point, the engine was allowed to reach thermal steady-state, confirmed when coolant and oil temperatures stabilized within ±2°C for at least 10 minutes. All data collection was initiated after stabilization to minimize thermal transients and ensure repeatability.

Ignition timing and throttle opening were kept constant across blends to isolate the effect of hydrogen enrichment. Fuel mass flow rates were adjusted to maintain consistent equivalence ratios ($\lambda \approx 1$) across test cases, measured using a gas flowmeter and corrected for ambient pressure and temperature.

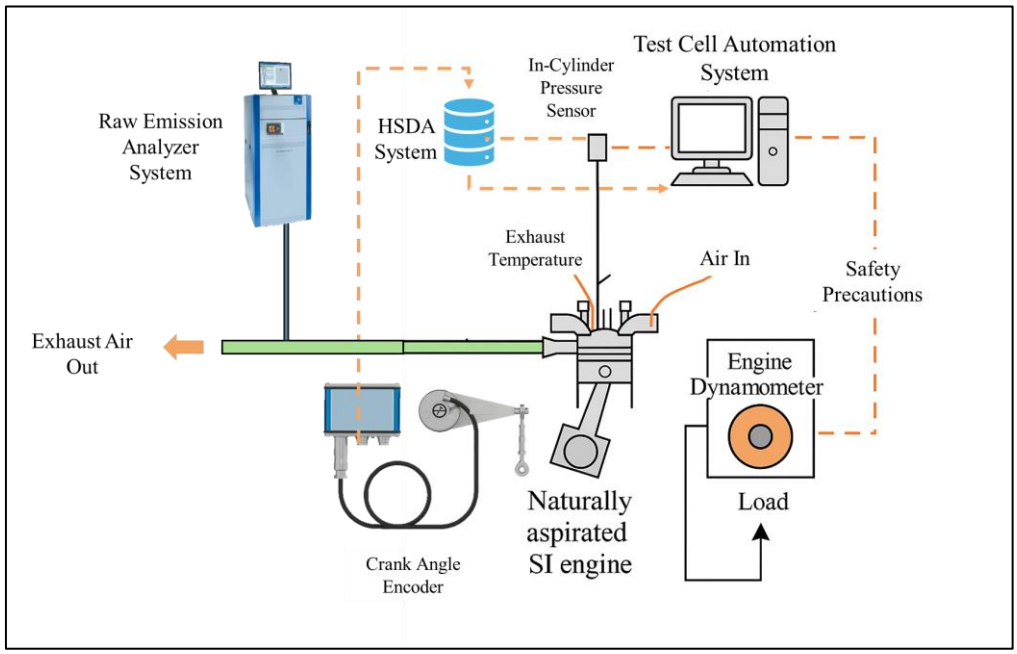

Figure 1. Experimental test setup with HSDA system for in-cylinder combustion analysis

3. IMPORTANCE OF KEY COMBUSTION PARAMETERS

Combustion analysis is central to understanding and optimizing the behaviour of SI engines operating HCNG blends [13]. Among the various diagnostic tools available, four combustion parameters are particularly critical for performance evaluation and control: in-cylinder pressure, HRR, MBF50, and combustion temperature. These parameters collectively determine how efficiently and cleanly fuel energy is converted into mechanical work and influence the development of combustion phasing strategies, emission control, and overall engine calibration [14].

3.1 In-cylinder pressure

In-cylinder pressure provides a direct measurement of combustion activity within the engine. It is a primary indicator of how combustion is initiated, propagated, and completed [15]. When hydrogen is added to natural gas, the resultant HCNG blend typically exhibits faster combustion due to hydrogen's higher flame speed and reactivity. This leads to an earlier and steeper pressure rise, with peak pressure occurring closer to Top Dead Centre (TDC). A higher peak pressure often translates to improved torque and thermal efficiency, provided that it remains within the mechanical limits of the engine [16].

Pressure curves also help assess the ignition delay and identify knock onset or abnormal combustion events. As hydrogen concentration increases, the pressure rise rate becomes sharper, which, while beneficial for performance, may necessitate advanced control of spark timing and intake temperature to prevent engine knock [17].

3.2 Heat Release Rate (HRR)

The HRR describes the rate at which chemical energy from the fuel is converted into thermal energy during combustion. It is derived from the time-resolved in-cylinder pressure and is a critical metric for understanding combustion intensity, duration, and stability [18].

HCNG blends generally show a pronounced increase in HRR, particularly in the premixed combustion phase. As hydrogen content increases, combustion duration typically shortens and the HRR curve becomes steeper and more peaked. These characteristics imply a more energetic and complete combustion process, which is beneficial for brake thermal efficiency [19]. However, overly rapid energy release can also elevate pressure gradients and thermal loads, necessitating precise ignition control and possibly exhaust gas recirculation for mitigation [20].

3.3 Mass fraction burned at 50% (MBF50)

MBF50, defined as the crank angle at which 50% of the fuel mass is combusted, serves as a prevalent metric for assessing combustion phasing. It delineates the temporal aspect of the principal energy release and exhibits a significant correlation with the overall efficiency of the engine. The optimal MBF50 generally resides within a restricted interval following TDC; any deviations on either flank may impair the efficacy of the power stroke [21].

In the context of hydrogen enrichment, the occurrence of MBF50 is typically advanced due to accelerated flame propagation. This advancement in combustion phasing has the potential to augment the effective expansion work, thereby enhancing efficiency [22]. Nevertheless, an excessively precocious MBF50 could result in detrimental work output or an escalation of knocking phenomena. Consequently, meticulous optimization of spark timing is imperative to ensure the alignment of MBF50 with the parameters of engine speed, load, and fuel characteristics [23].

3.4 Combustion temperature

The temperature within the combustion chamber is a key determinant of thermal efficiency and pollutant formation. Hydrogen's high calorific value and flame speed contribute to elevated combustion temperatures when added to CNG, particularly at stoichiometric or slightly lean air–fuel mixtures. These higher temperatures typically improve combustion completeness, reducing emissions of CO and Unburned Hydrocarbons (UHC) [24].

However, the increase in peak and average combustion temperatures also fosters the formation of Nitrogen Oxides (NO_x), which are highly temperature-sensitive pollutants. Additionally, sustained high in-cylinder temperatures may affect the long-term durability of pistons, valves, and cylinder heads, and increase the thermal load on cooling systems [25].

Estimating the combustion temperature in an indirect manner—typically utilizing thermodynamic models that rely on pressure readings and specific heat information—is crucial for achieving a balance between efficiency improvements, emissions regulations, and material durability [26]. In the realm of HCNG-powered engines, temperature patterns additionally act as an indicator for managing the risks associated with pre-ignition and surface ignition [27].

3.5 Interdependencies and application relevance

The four combustion parameters exhibit a profound interrelationship. For example, an elevated HRR results in heightened in-cylinder pressure and temperature, which subsequently influence the MBF50 and the phasing of combustion. Variations in hydrogen content exert considerable effects on all parameters, with even minimal alterations in blend ratios producing discernible changes in combustion characteristics [28].

In pragmatic terms, comprehending these interactions facilitates the formulation of refined ignition timing maps, fuel composition schedules, and adaptive control algorithms. In the context of multi-cylinder engines, these metrics further assist in the identification of cylinder-to-cylinder disparities and inform strategies for cylinder-specific calibration. Moreover, in engines functioning under varying load and speed conditions, these parameters underpin the execution of model-based predictive control systems that sustain combustion efficiency and ensure compliance with emission standards across all operational regimes [29].

Ultimately, the pressure inside the cylinder, HRR, mass burned fraction at 50% (MBF50), and combustion temperature constitute the essential analytical structure for assessing the feasibility of HCNG blends as sustainable options for SI engines [30]. Their detailed examination provides insights for both basic research and practical engine design.

4. COMBUSTION ANALYSIS UNDER VARYING LOAD CONDITIONS

4.1 Rate of Pressure Rise (RoPR)

The Rate of Pressure Rise (RoPR), expressed in bar per crank angle degree (bar/°CA), is a key indicator of combustion intensity and flame development speed within SI engines. It reflects how rapidly in-cylinder pressure increases as combustion progresses and is particularly important when analysing the effects of fuel reactivity and ignition timing. For HCNG-fueled engines, RoPR is influenced by hydrogen concentration, load condition, and combustion phasing, making it a sensitive metric for assessing combustion quality and knock propensity. The RoPR for the CNG and HCNG fuel blends at various BMEP levels is shown in Figure 2.

These results clearly demonstrate that hydrogen enrichment significantly elevates the peak pressure rise rate, particularly in mid- to high-load regimes. The largest relative increase in RoPR is observed at low load (1.5 BMEP), where hydrogen improves flame kernel stability and accelerates early combustion, effectively overcoming CNG's limitations in slow ignition and lean burn instability.

At higher loads (6.0 and 7.5 bar BMEP), all blends produce more intense combustion due to an increase in in-cylinder pressure and temperature. However, the incremental effect of hydrogen begins to plateau, suggesting that the combustion environment is already favourable and additional reactivity contributes less proportionally. The findings indicate that while hydrogen enrichment enhances combustion characteristics at lower loads, its benefits may diminish in more favourable combustion environments, necessitating further investigation into optimal blend ratios across varying operational conditions.

Figure 2 presents the variation in the rate of pressure rise (RoPR) as a function of crank angle for different HCNG blends (18%, 25%, and 30% hydrogen by volume) compared to conventional CNG, at four BMEP levels: 1.5, 3.7, 6.0, and 7.5 bar.

At low load (BMEP 1.5 bar), the peak RoPR for CNG is modest at 0.59 bar/°CA, reflecting the slow and incomplete combustion associated with lean burn and low in-cylinder temperatures. With hydrogen enrichment, RoPR increases to 0.69, 0.74, and 0.76 bar/°CA for 18HCNG, 25HCNG, and 30HCNG, respectively. These results confirm hydrogen's role in improving flame propagation and early-stage combustion under dilute conditions.

In the mid-load condition (BMEP 3.7 bar), RoPR grows significantly. CNG peaks at 1.10 bar/°CA, while 30HCNG reaches 1.54 bar/°CA—marking a ~40% increase. The flame speed enhancement due to hydrogen is more effective in this regime, where pressure and temperature conditions are sufficient to support rapid energy release. Similar enhancements have been documented by Bhasker and Porpatham in lean burn HCNG engines [31].

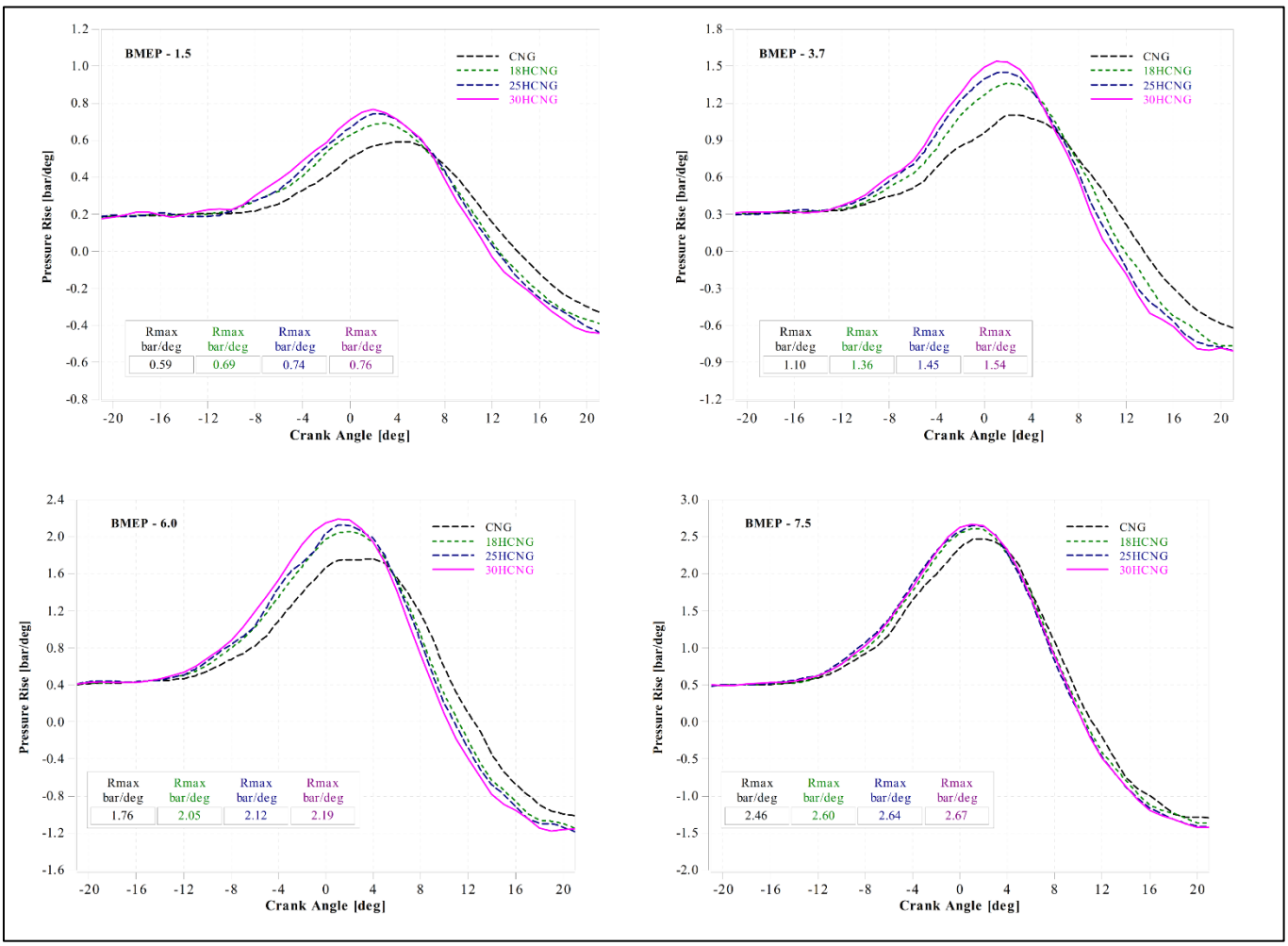

Figure 2. RoPR for CNG and HCNG blends under various BMEP conditions

At 6.0 bar BMEP, combustion intensity becomes more robust for all blends, with RoPR values rising to 1.76, 2.05, 2.12, and 2.19 bar/°CA for CNG, 18HCNG, 25HCNG, and 30HCNG, respectively. While the increment continues with hydrogen content, the marginal increase diminishes, suggesting that the combustion environment is nearing its optimal reactivity threshold. This trend aligns with De Simio et al., who observed a saturation effect in RoPR enhancement at high hydrogen fractions [18].

At full load (BMEP 7.5 bar), RoPR peaks at 2.67 bar/°CA for 30HCNG compared to 2.46 for CNG. The rate of increase is comparatively small, indicating diminishing returns due to already favourable ignition conditions. At this point, further increases in hydrogen concentration may necessitate spark retard or EGR strategies to avoid knock, as warned by Nitnaware and Suryawanshi [32].

Overall, RoPR increases with both hydrogen enrichment and BMEP. However, the influence of hydrogen is most pronounced at low and mid-loads and plateaus at high loads, underscoring the need for adaptive combustion control strategies for high hydrogen blends.

Knock margin analysis based on the rate of pressure rise

The RoPR is a crucial metric for assessing combustion intensity and knock susceptibility in spark-ignition engines. It serves as an early indicator of pressure oscillations and potential autoignition in the end-gas region. In this study, RoPR values were carefully analyzed across varying hydrogen blending ratios and engine loads, particularly focusing on the knock-prone full-load condition (BMEP = 7.5 bar).

Contrary to general concern for high hydrogen blends, the measured RoPR for the 30HCNG blend at 7.5 bar BMEP was 2.67 bar/°CA, only marginally higher than that of CNG (2.46 bar/°CA) under the same conditions. These values fall significantly below the typical knock-onset thresholds (8–10 bar/°CA) cited in literature for SI engines operating without EGR or knock-suppression strategies [33, 34]. Therefore, it is evident that even at full load, the 30HCNG blend exhibits stable combustion without entering the knock-limited regime.

The slightly higher RoPR for HCNG blends can be attributed to the enhanced laminar flame speed and thermal diffusivity of hydrogen, which accelerates combustion and leads to a steeper but still controlled pressure rise. This behaviour is further substantiated by the earlier MBF50 phasing observed in Section 4.3 and the elevated, yet stable, heat release rates and combustion temperatures discussed in Sections 4.2 and 4.4. Importantly, the pressure development remains within safe operational margins, demonstrating that hydrogen enrichment up to 30% vol. in CNG does not inherently induce knocking, at least under the current ignition phasing and mixture strategy.

Thus, the knock margin for all tested HCNG blends, including 30HCNG, is considered sufficient under the current combustion settings. These findings validate the potential of hydrogen addition in improving combustion dynamics without compromising knock resistance, provided that optimal spark timing and air–fuel ratios are maintained.

4.2 Heat Release Rate (HRR)

The HRR represents the rate at which chemical energy from the air–fuel mixture is converted into thermal energy within the combustion chamber. It is directly influenced by the fuel composition, ignition timing, flame speed, and in-cylinder turbulence. In SI engines, HRR serves as a critical metric for evaluating combustion intensity, speed, and efficiency [35]. Particularly for HCNG blends, HRR trends reveal important insights into how hydrogen affects the overall combustion process across varying engine loads [36].

The HRR is a key indicator of the energy conversion process within the combustion chamber. It reflects the rate at which chemical energy is transformed into thermal energy during combustion. In this study, the HRR was analyzed for four fuel blends—CNG, 18HCNG, 25HCNG, and 30HCNG—across four BMEP levels.

The normalised HRR trends, as illustrated in Figure 3, demonstrate a consistent and quantifiable increase in peak HRR values with rising hydrogen content across all load conditions. At 7.5 bar BMEP, 30HCNG showed the highest normalized HRR, followed by 25HCNG, 18HCNG, and CNG. A similar progression was observed at 6 bar, 3.7 bar and 1.5 bar BMEP levels, indicating that hydrogen enrichment consistently enhances the combustion intensity.

This improvement is attributable to the superior diffusivity, flame speed, and lower ignition energy of hydrogen, which enhance the overall combustion rate and shorten the combustion duration. Consequently, the combustion process becomes more complete and efficient, especially under lean and lower load conditions where CNG-only blends typically struggle due to slower flame propagation.

At a BMEP of 7.5 bar, the 30HCNG blend exhibited a pronounced spike in the HRR, a characteristic indicative of the highly reactive combustion dynamics inherent to hydrogen-enriched fuel mixtures under elevated load conditions. The inclusion of 30% hydrogen in the CNG blend significantly reduces ignition delay and enhances the laminar flame speed due to hydrogen's fundamental combustion properties—namely, low activation energy, high diffusivity, and high flame propagation rates. These features result in a rapid and concentrated combustion event near TDC, causing an abrupt and elevated HRR profile.

While such rapid combustion can enhance thermal efficiency, it also raises the risk of elevated pressure gradients or knock tendencies if not managed through appropriate spark timing or mixture control. These findings align with the established understanding of hydrogen combustion in spark ignition engines, wherein fuel reactivity increases disproportionately with higher hydrogen ratios, especially under high load conditions [33].

However, it is crucial to balance higher HRR with mechanical and thermal stress considerations. While higher HRR correlates positively with thermal efficiency, it also increases in-cylinder temperature and pressure gradients, which could risk engine knocking and increased NO_x emissions at elevated hydrogen concentrations. Studies by Ma et al. [37] affirm that optimal HRR supports improved indicated thermal efficiency but caution against excessive enrichment beyond stoichiometric limits due to potential detonation and durability concerns.

Based on the collected data and corroborated literature, an optimum HRR is likely achieved with 25–30% HCNG blends under medium to full-load conditions. This range provides a favourable trade-off between combustion stability, energy conversion, and mechanical safety.

Therefore, 25HCNG can be considered the optimal blend for most conditions, providing enhanced combustion without excessive pressure or thermal gradients. It enables improved engine efficiency, reduced misfire potential at low loads, and

robust operation at full load without exceeding safe limits for pressure rise or temperature.

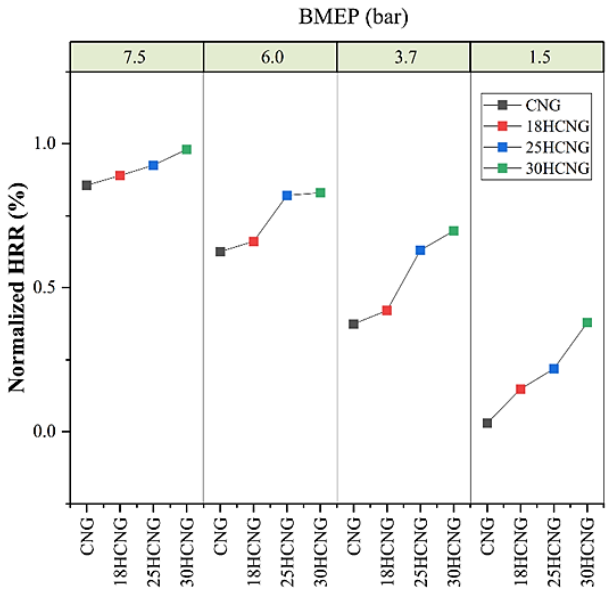

Figure 3. HRR for CNG and HCNG blends under various BMEP conditions

4.3 Combustion phasing – MBF50

MBF50 is the crank angle (or time) at which 50% of the fuel mass has been combusted, serving as a key indicator of combustion phasing. Accurate phasing ensures that the bulk of the energy release occurs during the most efficient portion of the expansion stroke, directly influencing torque output, thermal efficiency, and knock resistance [38].

A shift in MBF50 closer to TDC typically indicates a faster and more centered combustion event, contributing to higher thermal efficiency [39]. However, excessively advanced MBF50 can cause over-rapid pressure rise and increased knock propensity, while delayed MBF50 suggests inefficient combustion and greater heat losses [40].

An ideal MBF50 point often lies within 5–15° After Top Dead Center (ATDC) for optimum thermal efficiency and reduced emissions. In this study, MBF50 was measured across four different brake BMEP levels—1.5, 3.7, 6.0, and 7.5 bar—for CNG and three hydrogen-enriched HCNG blends (18HCNG, 25HCNG, and 30HCNG). The results are shown in Figure 4.

The results clearly demonstrate a consistent shift of MBF50 towards earlier phasing as hydrogen content increases. This trend becomes more prominent with increasing engine load. For instance, at BMEP 7.5 bar, MBF50 for CNG occurred at approximately 550 µs, whereas it advanced to around 430 µs for 30HCNG. To study combustion phasing analysis and to enable direct comparison with standard literature, MBF50 can be represented as crank angle degrees (°CA). For the tests conducted at 1500 RPM, 1°CA corresponds to 111 µs. Therefore, an MBF50 of 550 µs is equivalent to approximately 5°CA ATDC.

At low loads (1.5 bar), the combustion phasing was delayed for all fuels due to slower flame propagation, with CNG showing MBF50 at 1050 µs and 30HCNG at 700 µs. The enriched hydrogen content enhanced flame propagation speed and reduced ignition delay, aligning with the findings of Hora and Agarwal, who reported improved combustion characteristics with HCNG blends under varying compression ratios [41].

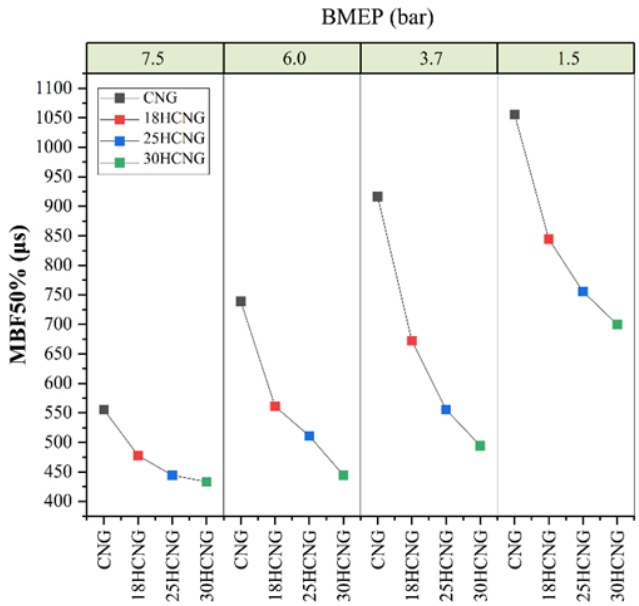

Figure 4. MBF50% in µs for CNG and HCNG blends under various BMEP conditions

This advancement in MBF50 is attributed to hydrogen's high diffusivity and low ignition energy, enabling faster kernel development and homogeneous flame propagation throughout the combustion chamber [42]. However, excessively advanced combustion phasing must be avoided, as it can lead to knocking tendencies or increased NO_x formation due to peak in-cylinder temperatures occurring too close to top dead center [43].

From a control strategy perspective, optimizing MBF50 through tailored spark timing becomes critical when varying HCNG ratios. Previous studies suggest that maintaining MBF50 within the window of 555µs–1333µs (i.e., 5–12° ATDC) is optimal for most HCNG engines to balance efficiency and combustion stability [44].

The MBF50 analysis confirms that hydrogen enrichment advances combustion phasing, improving efficiency and responsiveness. The 25HCNG blend offers the best compromise, delivering early yet controlled combustion across all load conditions. These results reinforce the importance of MBF50 as a combustion tuning metric, particularly when integrating alternative fuel blends into conventional SI engine platforms [45].

4.4 In-cylinder temperature

In-cylinder temperature is a critical outcome of the combustion process in SI engines. Though difficult to measure directly during engine operation, it is reliably inferred from combustion pressure traces, HRR profiles, and engine boundary conditions [45]. In the context of this study, in Figure 5, illustrates the variation of the in-cylinder temperature (Temp [K]) with crank angle for CNG and different hydrogen-enriched CNG (HCNG) blends. It also highlights how hydrogen enrichment in CNG influences both the magnitude and timing of the maximum combustion temperature under varying engine operating conditions. The normalized in-cylinder temperature trends were estimated based on the HRR

profiles corresponding to four engine load conditions: 1.5, 3.7, 6.0, and 7.5 bar BMEP.

The combustion of HCNG blends leads to elevated HRR peaks as hydrogen content increases. Given that hydrogen possesses a higher adiabatic flame temperature than methane and ignites more rapidly, this inherently leads to greater thermal energy generation within a shorter crank angle window [46]. The faster energy release contributes to a rise in peak and average in-cylinder temperatures, particularly at higher BMEPs.

Thermodynamic model for in-cylinder gas temperature estimation

The accurate estimation of mean in-cylinder gas temperature is essential for understanding the thermodynamic behaviour of combustion and assessing energy transfer characteristics in internal combustion engines, particularly when evaluating the impact of hydrogen-enriched fuels. In the present study, a quasi-steady, pressure-based thermodynamic model is implemented to determine the instantaneous mean gas temperature (T_i) from measured pressure and calculated in-cylinder volume profiles. The approach excludes surface heat losses and utilizes a variable polytropic exponent to reflect real-time changes in gas thermodynamic properties during combustion.

The procedure begins with calculating the in-cylinder gas mass mmm, derived using the ideal gas law based on intake manifold conditions. The expression for inducted charge is:

$$m = I.V_H \frac{P_s}{R.T_s} \tag{1}$$

where, I is the volumetric efficiency (typically 0.9), V_H the swept volume, P_s and T_s the intake pressure and temperature, and R the specific gas constant (287.12 J/kg·K). This standard intake-based estimation aligns with formulations established in foundational thermodynamic texts, including Heywood [47].

To further resolve the thermodynamic state of the cylinder, the apparent heat release Q_i is estimated using a single-zone formulation that incorporates a variable polytropic exponent κ_i, improving the fidelity of HRR analysis over fixed-κ models:

$$Q_i = \frac{\kappa_i}{\kappa_i - 1} V_{i+\frac{n}{2}} \left[P_{i+\frac{n}{2}} - P_{i-\frac{n}{2}} \left(\frac{V_i}{V_{i+\frac{n}{2}}} \right)^{\kappa_i} \right] (X_i + 1) \tag{2}$$

Here, X_i denotes an engine-type factor (0 for spark-ignition engines, 1 for compression-ignition), and n is the crank angle interval (1°CA in this case). This approach is grounded in thermodynamic principles detailed by Brunt and Platts, who emphasize its applicability for high-resolution combustion analysis in diesel engines [48].

A crucial feature of the model is the dynamic computation of the polytropic coefficient κ_i, which adapts to temperature-induced variations in specific heat at constant volume (C_{vi}). This coefficient is modelled empirically as:

$$C_{vi} = 0.7 + T_i.(0.155 + A_i).10^{-3} \tag{3}$$

$$\kappa_i = \frac{0.2888}{C_{vi}} + 1 \tag{4}$$

where, A_i is a correction factor depending on engine type, as described by Krieger and Borman [49]. This dynamic approach captures gas-specific heat variations due to combustion product composition and temperature levels.

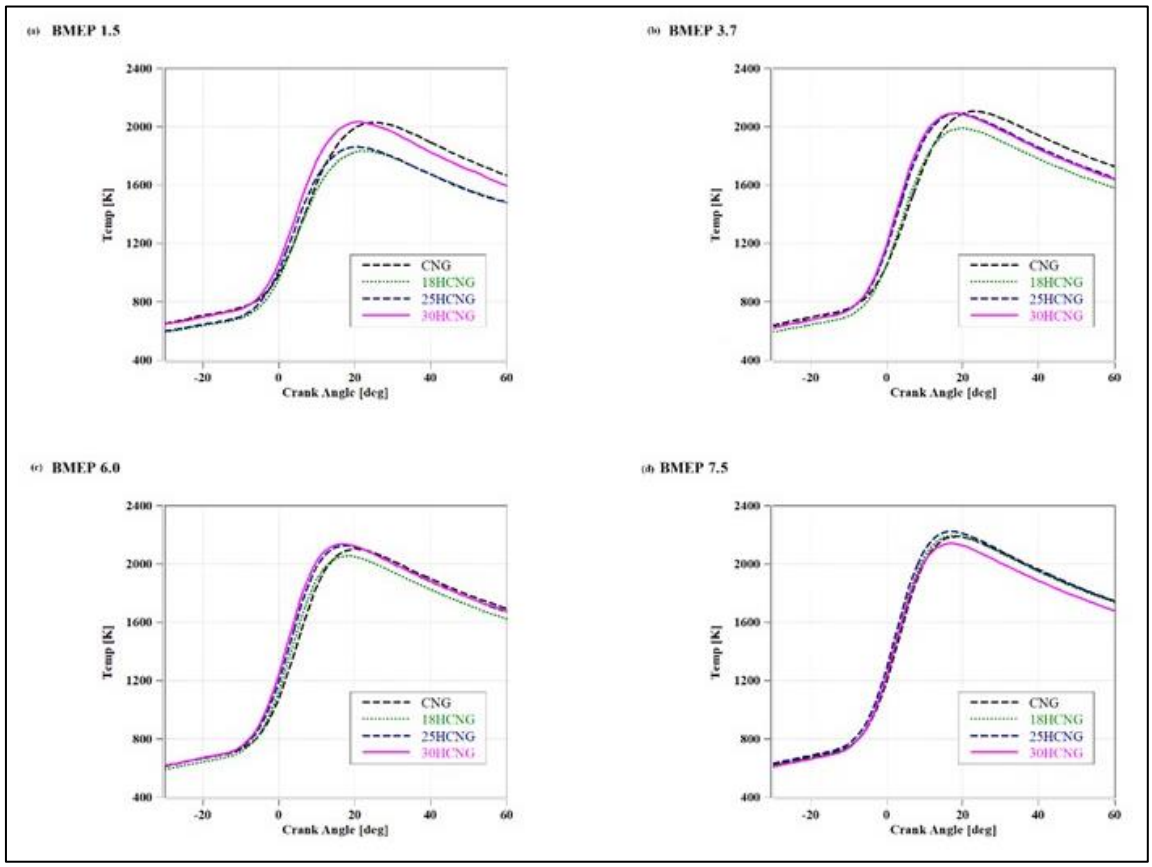

Figure 5. Combustion temperature for CNG and HCNG blends under various BMEP conditions

The final step in the process involves calculating the instantaneous mean gas temperature using the rearranged ideal gas law:

$$T_i = \frac{P_i.V_i}{m.R.(1+X_i)} \quad (5)$$

This formulation enables direct tracking of the thermal state during the engine cycle and differentiates between SI and CI operation through the inclusion of X_i. The result is a robust framework capable of resolving combustion phasing, heat release trends, and thermal NO_x potential with high temporal accuracy.

The reliability of this model is further validated through alignment with literature-based modelling strategies. Gatowski et al. confirmed the application of polytropic HRR methods in spark-ignition engines [50], while Cheung and Heywood verified mean temperature estimates using production engine pressure data [51]. Additionally, Eriksson and Andersson established analytical pressure modelling frameworks that complement the proposed formulation [52].

Figure 5 illustrates the combustion temperature as a function of crank angle for CNG and three HCNG blends (18%, 25%, and 30%) under four BMEP conditions (1.5, 3.7, 6.0, and 7.5 bar).

The results reveal a consistent increase in peak combustion temperature with hydrogen enrichment across all load conditions. At 1.5 bar BMEP, the peak in-cylinder temperature rises from ~1920 K for CNG to ~2040 K for 30HCNG. This thermal increment continues at higher loads, with the peak temperature at 7.5 bar approaching ~2280 K for 30HCNG compared to ~2120 K for baseline CNG. This trend is attributable to hydrogen's higher laminar flame speed and faster chemical kinetics, which result in shorter combustion durations and faster heat release near TDC. This effect was also confirmed by Varma and Mittal, who observed significant increases in in-cylinder temperatures with HCNG blending due to accelerated flame propagation and enhanced combustion efficiency [53].

Interestingly, while the instantaneous HRR increases with hydrogen addition, the cumulative heat release remains comparable across blends. This suggests that hydrogen primarily reshapes the combustion profile, concentrating energy release closer to TDC, rather than changing the total chemical energy released. These changes lead to more efficient expansion and higher Indicated Mean Effective Pressure (IMEP), particularly at mid- to high-load conditions.

At low loads (e.g., 1.5 bar BMEP), the relative benefit of hydrogen is more pronounced due to the otherwise sluggish flame propagation with pure CNG. In such conditions, HCNG blends significantly raise the in-cylinder temperature early in the combustion cycle, thereby promoting more stable flame propagation. This aligns with findings by Farhan et al., who reported that HCNG usage improves early combustion stability and thermal loading in lean-burn SI engines [54].

However, the rise in peak in-cylinder temperature can increase thermal NO_x formation, necessitating careful optimization of spark timing and Exhaust Gas Recirculation (EGR) strategies. This thermal penalty highlights the need to balance combustion efficiency with emission control, particularly at high hydrogen blends and elevated loads.

In summary, the integration of 25–30% hydrogen by volume in CNG results in a marked increase in peak combustion temperature and quicker energy release, which enhances overall combustion quality and engine thermal efficiency. Nevertheless, these gains must be counterbalanced with appropriate after-treatment or in-cylinder control techniques to manage potential NO_x emissions.

5. PERFORMANCE AND EMISSION ANALYSIS OF HCNG BLENDS

This section evaluates the performance and emission behavior of a multi-cylinder SI engine fueled with varying HCNG blends across four load conditions, corresponding to BMEP levels of 1.5, 3.7, 6.0, and 7.5 bar. The performance metric considered is BSFC, and the emissions assessed include CO, HC, and NO_x.

5.1 Brake Specific Fuel Consumption (BSFC)

The BSFC data shown in Figure 6 clearly indicates that hydrogen enrichment contributes to enhanced combustion efficiency across all loads. At full load (7.5 bar BMEP), BSFC reduces by 3% from 219.81 g/kWh (CNG) to 212.73 g/kWh (30HCNG). Similarly, the lowest load (1.5 bar) shows a drop of 8% from 429.75 g/kWh to 393.93 g/kWh with increasing hydrogen content.

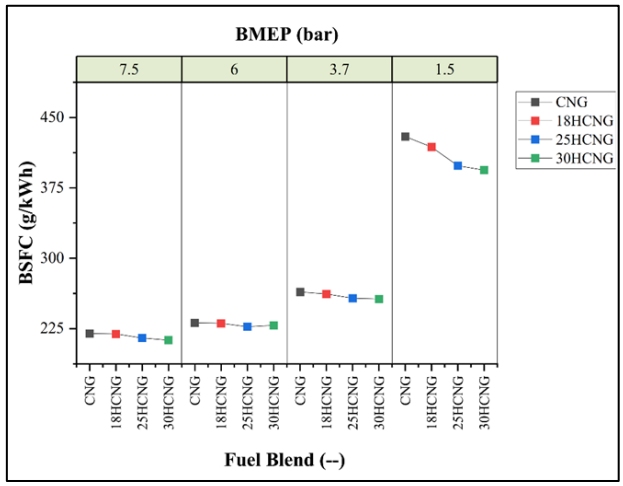

Figure 6. BSFC for CNG and HCNG blends under various BMEP conditions

This improvement is attributed to the higher HRR and more advanced MBF50 phasing achieved with HCNG blends. Hydrogen accelerates flame propagation and ensures more complete combustion near TDC, leading to faster and denser heat release, as evidenced in Sections 4.2 and 4.3. Furthermore, the increased in-cylinder temperature with HCNG (Section 4.4) improves vaporization and reduces combustion duration, contributing to better thermal conversion efficiency. Similar reductions in BSFC with HCNG were reported by Saleh and Mahmood, who observed up to 8% improvements in a comparable multi-cylinder SI engine operating with 30% hydrogen blends [55].

5.2 Carbon Monoxide (CO) emissions

In raw exhaust emission measurements, CO is quantified on a dry basis, meaning the water vapour is first removed from the sample to ensure accuracy in measuring non-condensable gases. This practice, standardized under ISO 8178-1:2020, ensures consistency in legislative compliance for gaseous

emissions. The CO emissions, evident from Figure 7, show a non-linear reduction with increasing hydrogen content at medium and high BMEP values. For example, at 6.0 bar BMEP, CO decreases from 51.34 ppm (CNG) to 31.90 ppm (30HCNG), reflecting improved oxidation efficiency due to the enhanced local equivalence ratio and superior flame speed of hydrogen.

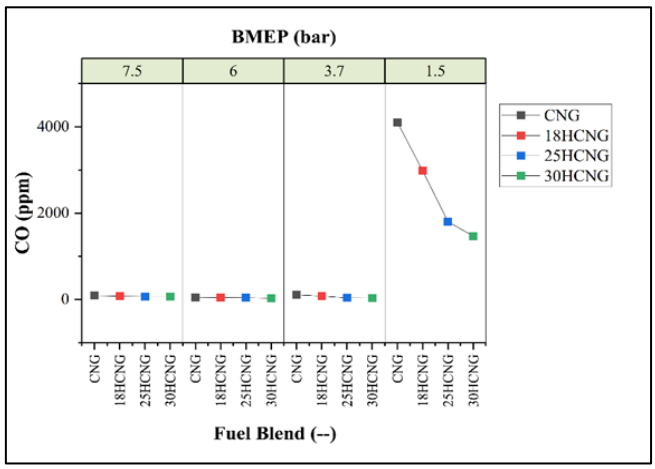

Figure 7. CO emissions for CNG and HCNG blends under various BMEP conditions

However, at 1.5 bar BMEP, CO emissions spike drastically to 4102.28 ppm for CNG and remain high even with 30HCNG (1468.70 ppm). This increase is closely linked to poor combustion conditions at low load, where lower temperatures and turbulence result in quenching and incomplete oxidation. Despite the improved MBF50 and modest RoPR gains observed at 1.5 bar with HCNG, the low in-cylinder temperatures and lean stratification limit the benefit. The relationship between low-load inefficiency and high CO has been well-documented in literature, notably by Shahid et al., emphasizing the need for intake heating or throttling strategies [34].

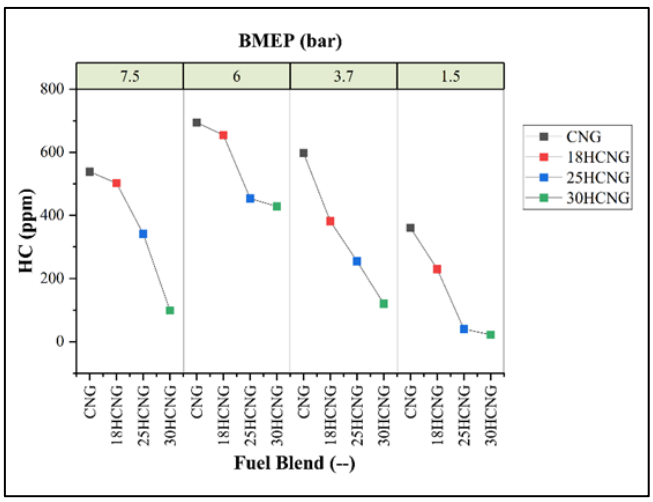

Figure 8. HC emissions for CNG and HCNG blends under various BMEP conditions

5.3 Hydrocarbon (HC) emissions

In raw exhaust emission measurements, HC is quantified on a wet basis, where the exhaust sample retains its moisture content to correctly capture water-soluble components such as unburnt hydrocarbons. This practice, standardized according to ISO 8178-1:2020, ensures consistent compliance with regulations regarding gaseous emissions. HC emissions follow a strong downward trend with increasing hydrogen concentration, as seen from Figure 8. At 7.5 bar BMEP, HC drops from 538.15 ppm (CNG) to 98.81 ppm (30HCNG)—an ~82% reduction. This trend is mirrored at all load levels, with the sharpest declines occurring from 18HCNG to 25HCNG.

This behaviour directly correlates with the higher HRR and steeper pressure rise noted in Section 4.1, which promotes full combustion and reduces quenching in boundary layers. Faster combustion with hydrogen ensures fewer UHC escape into the exhaust, especially under lean and transient conditions. Furthermore, the higher peak temperatures observed for HCNG blends (Section 4.4) support more effective cracking and oxidation of intermediate hydrocarbons.

5.4 Nitrogen Oxides (NO_x) emissions

In raw exhaust emission measurements, Nitrogen Oxides (NOx) are quantified on a wet basis to maintain moisture content, which is essential for accurately capturing water-soluble components like unburned Nitrogen Oxides. This method follows ISO 8178-1:2020 standards to ensure compliance with gaseous emissions regulations. The NO_x emissions shown in Figure 9 exhibits a dual trend. At higher BMEP levels, NO_x emissions decrease significantly, from 8.25 ppm (CNG) to 1.40 ppm (30HCNG) at 7.5 bar. This decline is counterintuitive, given that HCNG increases combustion temperature. This is primarily due to cooler post-flame temperatures induced by leaner mixtures and lower residuals. However, it can be explained by the shorter combustion duration and faster phasing (MBF50), which reduces the residence time for NOx formation in high-temperature zones.

At lower loads (1.5 and 3.7 bar), NO_x emissions increase with hydrogen addition. For instance, NO_x rises from 0.88 ppm (CNG) to 3.27 ppm (30HCNG) at 1.5 bar. This is attributed to the rapid combustion onset and local temperature spikes associated with the early heat release of hydrogen, as evidenced in the MBF50 trends.

These dual behaviours align with known combustion chemistry, where NO_x formation is not solely a function of peak temperature but also residence time, oxygen availability, and post-flame cooling rates. Similar results were found in the work of Shahid et al., reinforcing the importance of tailored spark timing and EGR strategies when operating HCNG blends across diverse load ranges [34].

This deviation is attributed to localized high-temperature zones formed due to hydrogen's fast flame speed and enhanced diffusivity, even under otherwise globally lean and cold combustion environments. Under such conditions, turbulent eddies and flame stretch create small-scale rich pockets where local stoichiometry approaches or exceeds unity. These micro-environments facilitate thermal NO_x formation via the Zeldovich mechanism, despite low average in-cylinder temperatures.

Furthermore, hydrogen addition promotes early flame kernel development, which reduces ignition delay and pushes the heat release closer to TDC, increasing the peak temperature gradients within the flame front. These kinetically active fronts, rich in radicals like O, H, and OH, accelerate the NO_x-forming chain reactions, particularly in zones of flame curvature and stratification [56, 57].

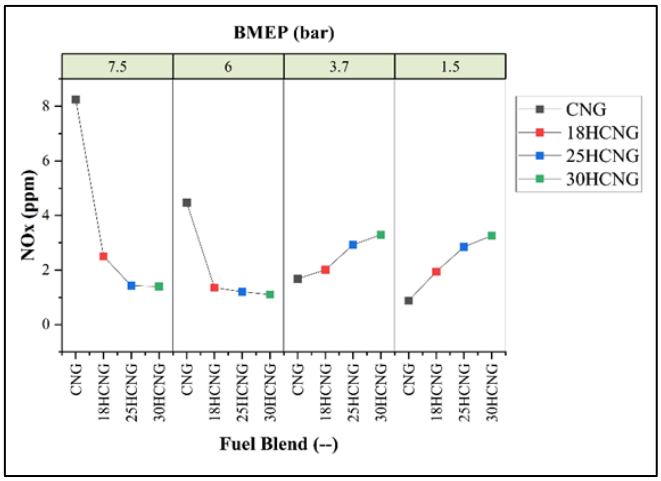

Figure 9. NOx emissions for CNG and HCNG blends under various BMEP conditions

Hence, while the overall cylinder bulk temperature remains low, chemical kinetics coupled with turbulent flame-flame interactions result in spatially constrained but thermally dominant NO_x regions under high-H_2, low-load conditions. Similar localised NO_x behaviour under dilute hydrogen combustion regimes has been experimentally observed in prior studies [58].

The overall performance-emission matrix demonstrates that hydrogen enrichment in CNG (particularly 25–30%) offers significant benefits in thermal efficiency and emission reductions under medium and high load conditions. However, low-load performance remains challenged by CO and NO_x sensitivities, necessitating adaptive combustion control to fully exploit HCNG's potential across the operational envelope.

6. RESULTS AND CONCLUSIONS

This study systematically evaluates the influence of HCNG blends—18%, 25%, and 30% by volume—on the combustion characteristics, engine performance, and emission profile of a naturally aspirated, multi-cylinder SI engine operated across four distinct load conditions (BMEP: 1.5, 3.7, 6.0, and 7.5 bar). The experimental results, analyzed through key combustion parameters such as RoPR, HRR, MBF50 (combustion phasing), and in-cylinder temperature, were critically correlated with BSFC and gaseous emissions (CO, HC, NO_x). The major findings and their implications are as follows:

6.1 Combustion trends

Hydrogen addition resulted in a consistent enhancement of combustion characteristics across all blends and load conditions:

i. Rate of Pressure Rise (RoPR) increased significantly with hydrogen enrichment due to accelerated flame propagation and improved combustion reactivity. The RoPR gain was most prominent between 0–25% hydrogen, peaking at 2.67 bar/°CA for 30HCNG at 7.5 bar BMEP, compared to 2.46 bar/°CA for CNG, indicating more rapid and energetic combustion.

ii. HRR curves shifted earlier and became sharper for HCNG blends. The cumulative heat release remained largely comparable across blends, confirming that hydrogen reshapes the combustion profile without altering total energy content. This early and rapid combustion resulted in more work extraction near TDC.

iii. MBF50 values advanced with higher hydrogen ratios, indicating earlier combustion phasing. For instance, MBF50 at 30HCNG under full load occurred approximately 20–25% sooner than with CNG, signifying better thermodynamic timing for peak pressure development.

iv. In-cylinder temperatures rose with hydrogen enrichment, particularly at mid-to-high loads, facilitating more complete oxidation of hydrocarbons and reducing ignition delay.

6.2 Performance evaluation

Hydrogen enrichment demonstrated a clear advantage in thermal efficiency as reflected in BSFC.

i. BSFC consistently decreased with higher hydrogen content. At 7.5 bar BMEP, the value dropped from 219.81 g/kWh (CNG) to 212.73 g/kWh (30HCNG), with similar trends across lower loads. These gains are linked to faster combustion (higher HRR and RoPR) and reduced combustion duration (advanced MBF50), confirming hydrogen's effectiveness in improving thermal conversion.

ii. At lower loads, the combustion benefits were less pronounced due to inherently lower in-cylinder pressures and turbulence. Nevertheless, hydrogen still improved combustion efficiency over baseline CNG.

6.3 Emission behaviour

The emission profile of the engine responded variably to hydrogen addition:

i. CO and HC emissions decreased sharply with hydrogen enrichment due to improved combustion completeness and higher in-cylinder temperatures. HC, in particular, dropped by over 80% at full load from 538.15 ppm (CNG) to 98.81 ppm (30HCNG).

ii. NO_x emissions exhibited a dual trend:
   - At high loads, NO_x reduced due to shortened residence times and a leaner burn despite increased temperatures.
   - At low loads, NO_x rose with hydrogen addition due to localized high-temperature zones created by rapid combustion and advanced ignition timing.

This suggests that while HCNG is cleaner in terms of incomplete combustion products (CO, HC), NO_x control requires careful optimization—such as EGR or retarded spark timing—especially under light-load conditions. The results confirm that HCNG blends up to 30% hydrogen can substantially improve combustion quality, engine thermal efficiency, and emission performance under steady-state operation in SI engines. Among the blends, 25HCNG emerged as the optimal formulation, balancing combustion intensity, thermal efficiency, and emissions across all load conditions.

The interdependence between combustion behaviour and engine output metrics underscores the importance of integrating combustion analysis into performance evaluation. HCNG's faster burn rate and earlier phasing contribute directly to lower fuel consumption and lower HC/CO emissions. However, thermal NO_x behaviour is sensitive to load and hydrogen content, warranting load-dependent calibration strategies.

This study presents a comprehensive combustion analysis

of a spark-ignition engine fueled with HCNG blends across varying BMEP conditions. The experimental findings affirm that HCNG offers significant advantages in terms of combustion phasing, HRR, and RoPR, particularly under partial and low-load conditions. Combustion analysis revealed that the 25% HCNG blend offered the most optimal trade-off, achieving improved MBF50 timing, reduced HRR delay, and minimal RoPR fluctuations while maintaining operation well below the knock margin even at full load (7.5 bar BMEP). Moreover, performance assessments such as BSFC also favoured 25% HCNG, supported by concurrent emission reductions in CO and HC.

While 30% HCNG showed further reductions in HC emissions and enhanced laminar flame speed, it also exhibited a marginal increase in RoPR and elevated peak temperatures at high load. Though still under knock-prone limits, the aggressive combustion behaviour slightly offset its BSFC and emission benefits compared to 25% HCNG.

Notably, Kalsi & Subramanian concluded that 30% HCNG performed best in a biodiesel-fueled RCCI engine, contrasting with the results derived from spark-ignition (SI) mode with stoichiometric fuelling. Their RCCI setup benefits from stratified combustion and late diesel injection strategies, inherently more tolerant of higher hydrogen fractions due to their dual-fuel mode and in-cylinder mixing [8]. In contrast, the homogeneous SI setup in this study imposes greater sensitivity to hydrogen's high flame speed and autoignition tendencies, making 25% HCNG a more balanced and stable choice under standard ignition strategies.

Thus, the observed discrepancy underscores the influence of engine operating mode, fuel reactivity control, and load strategies on HCNG's optimal concentration.

In future studies, incorporation of EGR, variable spark timing, and closed-loop control can be explored to extend HCNG applicability across transient operating modes and real-world drive cycles.

REFERENCES

[1] Han, Z., Wu, Z., Huang, Y., Shi, Y., Liu, W. (2021). Impact of natural gas fuel characteristics on the design and combustion performance of a new light-duty CNG engine. International Journal of Automotive Technology, 22: 1619-1631. https://doi.org/10.1007/s12239-021-0140-1

[2] Hwang, J., Maharjan, K., Cho, H. (2023). A review of hydrogen utilization in power generation and transportation sectors: Achievements and future challenges. International Journal of Hydrogen Energy, 48(74): 28629-28648. https://doi.org/10.1016/j.ijhydene.2023.04.024

[3] Nguyen, T.H., Balasubramanian, D., Inbanaathan, P.V., Le, T.T., Le, H.C., Truong, T.H., Cao, D.N. (2025). A comprehensive review of compressed natural gas (CNG)-fueled engines under different operating conditions and combustion strategies on performance and combustion characteristics. Energy & Environment, 36(3): 0958305X251315402. https://doi.org/10.1177/0958305X251315402

[4] Trivedi, S., Prasad, R., Mishra, A., Kalam, A., Yadav, P. (2020). Current scenario of CNG vehicular pollution and their possible abatement technologies: An overview. Environmental Science and Pollution Research, 27: 39977-40000. https://doi.org/10.1007/s11356-020-10361-7

[5] Prasad, R.K., Mustafi, N., Agarwal, A.K. (2020). Effect of spark timing on laser ignition and spark ignition modes in a hydrogen enriched compressed natural gas fuelled engine. Fuel, 276: 118071. https://doi.org/10.1016/j.fuel.2020.118071

[6] Prasad, R.K., Jain, S., Verma, G., Agarwal, A.K. (2017). Laser ignition and flame kernel characterization of HCNG in a constant volume combustion chamber. Fuel, 190: 318-327. https://doi.org/10.1016/j.fuel.2016.11.003

[7] Patil, K.R., Khanwalkar, P.M., Thipse, S.S., Kavathekar, K.P., Rairikar, S.D. (2009). Development of HCNG blended fuel engine with control of NOx emissions. In 2009 Second International Conference on Emerging Trends in Engineering & Technology, Nagpur, India, pp. 1068-1074. https://doi.org/10.1109/ICETET.2009.81

[8] Kalsi, S.S., Subramanian, K.A. (2017). Experimental investigations of effects of hydrogen blended CNG on performance, combustion and emissions characteristics of a biodiesel fueled reactivity controlled compression ignition engine (RCCI). International Journal of Hydrogen Energy, 42(7): 4548-4560. https://doi.org/10.1016/j.ijhydene.2016.12.147

[9] Mustafi, N.N., Agarwal, A.K. (2020). Combustion and emission characteristics, and emission control of CNG fueled vehicles. In Alternative Fuels and Their Utilization Strategies in Internal Combustion Engines. Springer, Singapore. https://doi.org/10.1007/978-981-15-0418-1_12

[10] Luo, S., Ma, F., Mehra, R.K., Huang, Z. (2020). Deep insights of HCNG engine research in China. Fuel, 263: 116612. https://doi.org/10.1016/j.fuel.2019.116612

[11] Khab, H., Chaker, A., Ziani, L. (2019). Effects of pressure and hydrogen addition to methane on the temperatures within a pressurized cylinder during the vehicle refueling of HCNG. International Journal of Hydrogen Energy, 44(39): 22437-22444. https://doi.org/10.1016/j.ijhydene.2019.04.209

[12] Prasad, R.K., Agarwal, A.K. (2021). Development and comparative experimental investigations of laser plasma and spark plasma ignited hydrogen enriched compressed natural gas fueled engine. Energy, 216: 119282. https://doi.org/10.1016/j.energy.2020.119282

[13] Juknelevičius, R., Mehra, R.K., Ma, F., Szwaja, S. (2018). In-cylinder combustion analysis of a SI engine fuelled with hydrogen enriched compressed natural gas (HCNG): Engine performance, efficiency and emissions. Journal of KONES, 25(3): 253-260.

[14] Maurya, R.K. (2019). Combustion Characteristic Analysis. In: Reciprocating Engine Combustion Diagnostics. Mechanical Engineering Series. Springer, Cham. https://doi.org/10.1007/978-3-030-11954-6_7

[15] Catalani, I., Bosi, L., Baroni, A., Romani, L., Vichi, G., Bellissima, A., Asai, G., Minamino, R., Ferrara, G. (2022). In-cylinder pressure estimation in a multi-cylinder engine by combining the instantaneous crankshaft speed data and a 0D thermodynamic model. Numerical validation. Journal of Physics: Conference Series, 2385(1): 012069. https://doi.org/10.1088/1742-6596/2385/1/012069

[16] Luo, H., Chang, F., Jin, Y., Ogata, Y., Matsumura, Y., Ichikawa, T., Kim, W., Nakashimada, Y., Nishida, K. (2021). Experimental investigation on performance of

hydrogen additions in natural gas combustion combined with CO_2. International Journal of Hydrogen Energy, 46(70): 34958-34969. https://doi.org/10.1016/j.ijhydene.2021.08.037
[17] Goto, J., Kobashi, Y., Matsumura, Y., Shibata, G., Ogawa, H., Kuragaki, N. (2022). Spark knock suppression in spark ignition engines with hydrogen addition under low and high engine speeds. International Journal of Hydrogen Energy, 47(41): 18169-18181. https://doi.org/10.1016/j.ijhydene.2022.03.286
[18] De Simio, L., Iannaccone, S., Guido, C., Napolitano, P., Maiello, A. (2024). Natural Gas/Hydrogen blends for heavy-duty spark ignition engines: Performance and emissions analysis. International Journal of Hydrogen Energy, 50: 743-757. https://doi.org/10.1016/j.ijhydene.2023.06.194
[19] Mariani, A., Unich, A., Minale, M. (2019). Methane/Hydrogen blends in controlled auto ignition engines with EGR: Evaluation of NOx emissions. Chemical Engineering Transactions, 76: 301-306. https://doi.org/10.3303/CET1974051
[20] Pizzonia, F., Castiglione, T., Bova, S. (2016). A Robust Model Predictive Control for efficient thermal management of internal combustion engines. Applied Energy, 169: 555-566. https://doi.org/10.1016/j.apenergy.2016.02.063
[21] Federico Stola, V.R., De Cesare, M., Ponti, F. (2020). Method of estimating the MFB50 combustion index generated by the cylinders of an internal combustion engine. EP3 171 006B1.
[22] Karimkashi, S., Kaario, O., Vuorinen, V. (2022). Effects of hydrogen enrichment and turbulence intensity on the combustion mode in locally stratified dual-fuel mixtures of n-dodecane/methane. Applications in Energy and Combustion Science, 10: 100072. https://doi.org/10.1016/j.jaecs.2022.100072
[23] Kou, Y., Gao, Y., You, Y., Wang, Y. (2022). Optimization of a spark ignition engine knock and performance using the epsilon-constrained differential evolution algorithm and multi-objective differential evolution algorithm. ACS Omega, 7(36): 31638-31650. https://doi.org/10.1021/acsomega.1c06678
[24] Kakoee, A., Bakhshan, Y., Aval, S.M., Gharehghani, A. (2018). An improvement of a lean burning condition of natural gas/diesel RCCI engine with a pre-chamber by using hydrogen. Energy Conversion and Management, 166: 489-499. https://doi.org/10.1016/j.enconman.2018.04.063
[25] Krakowski, R. (2012). Effect of elevated coolant temperature on the exhaust composition of piston internal-combustion engine. Journal of KONES, 19: 263-270. https://doi.org/10.5604/12314005.1137932
[26] Abdullah, A.A., Al-Tayyar, M.A., Bachache, H.K. (2022). A temperature measuring of combustion machinery systems using light absorbing of gas. AIP Conference Proceedings, 2386(1): 040037. https://doi.org/10.1063/5.0067548
[27] Afkhami, B., Kakaee, A.H., Pouyan, K. (2012). Studying engine cold start characteristics at low temperatures for CNG and HCNG by investigating low-temperature oxidation. Energy Conversion and Management, 64: 122-128. https://doi.org/10.1016/j.enconman.2012.04.016
[28] Moreno, F., Arroyo, J., Muñoz, M., Monné, C. (2012). Combustion analysis of a spark ignition engine fueled with gaseous blends containing hydrogen. International Journal of Hydrogen Energy, 37(18): 13564-13573. https://doi.org/10.1016/j.ijhydene.2012.06.060
[29] Fussey, P. (2014). Automotive combustion modelling and control. Doctoral dissertation, Oxford University, UK.
[30] Dhyani, V., Subramanian, K.A. (2019). Experimental based comparative exergy analysis of a multi-cylinder spark ignition engine fuelled with different gaseous (CNG, HCNG, and hydrogen) fuels. International Journal of Hydrogen Energy, 44(36): 20440-20451. https://doi.org/10.1016/j.ijhydene.2019.05.229
[31] Bhasker, J.P., Porpatham, E. (2017). Effects of compression ratio and hydrogen addition on lean combustion characteristics and emission formation in a Compressed Natural Gas fuelled spark ignition engine. Fuel, 208: 260-270. https://doi.org/10.1016/j.fuel.2017.07.024
[32] Nitnaware, P.T., Suryawanshi, J.G. (2016). Effects of MBT spark timing on performance emission and combustion characteristics of SI engine using hydrogen-CNG blends. International Journal of Hydrogen Energy, 41(1): 666-674. https://doi.org/10.1016/j.ijhydene.2015.11.074
[33] Karim, G.A. (2003). Hydrogen as a spark ignition engine fuel. International Journal of Hydrogen Energy, 28(5): 569-577. https://doi.org/10.1016/S0360-3199(02)00150-7
[34] Shahid, M.I., Chen, T., Farhan, M., Rao, A., Salam, H.A., Xiao, Q., Ma, F., Li, X. (2025). Experimental study of emissions and conversion efficiency analysis of hydrogen-enriched compressed natural gas engine before and after catalytic converter and predicted by improved particle swarm optimization in conjunction with back propagation neural network (IMPSO-BPNN). Energy, 315: 134409. https://doi.org/10.1016/j.energy.2025.134409
[35] Martinka, J., Rantuch, P., Martinka, F., Wachter, I., Štefko, T. (2023). Improvement of heat release rate measurement from woods based on their combustion products temperature rise. Processes, 11(4): 1206. https://doi.org/10.3390/pr11041206
[36] Ma, F., Wang, M., Jiang, L., Deng, J., Chen, R., Naeve, N., Zhao, S. (2010). Performance and emission characteristics of a turbocharged spark-ignition hydrogen-enriched compressed natural gas engine under wide open throttle operating conditions. International Journal of Hydrogen Energy, 35(22): 12502-12509. https://doi.org/10.1016/j.ijhydene.2010.08.053
[37] Ma, F., Wang, M., Jiang, L., Chen, R., Deng, J., Naeve, N., Zhao, S. (2010). Performance and emission characteristics of a turbocharged CNG engine fueled by hydrogen-enriched compressed natural gas with high hydrogen ratio. International Journal of Hydrogen Energy, 35(12): 6438-6447. https://doi.org/10.1016/j.ijhydene.2010.03.111
[38] Ponti, F., Ravaglioli, V., Moro, D., Serra, G. (2013). *MFB50* on-board estimation methodology for combustion control. Control Engineering Practice, 21(12): 1821-1829. https://doi.org/10.1016/j.conengprac.2013.05.001
[39] Anetor, L., Osakue, E.E., Odetunde, C. (2017). Combustion dynamics at the top dead center position of

a spark ignition engine. FME Transactions, 45(4): 548-558. https://doi.org/10.5937/fmet1704548A
[40] Ponti, F., Ravaglioli, V., Moro, D., Serra, G. (2010). Combustion control using a model-based MFB50 estimation methodology. IFAC Proceedings Volumes, 43(7): 282-287. https://doi.org/10.3182/20100712-3-DE-2013.00122
[41] Hora, T.S., Agarwal, A.K. (2016). Effect of varying compression ratio on combustion, performance, and emissions of a hydrogen enriched compressed natural gas fuelled engine. Journal of Natural Gas Science and Engineering, 31: 819-828. https://doi.org/10.1016/j.jngse.2016.03.041
[42] Srivastava, D.K., Agarwal, A.K. (2014). Comparative experimental evaluation of performance, combustion and emissions of laser ignition with conventional spark plug in a compressed natural gas fuelled single cylinder engine. Fuel, 123: 113-122. https://doi.org/10.1016/j.fuel.2014.01.046
[43] Di Iorio, S., Sementa, P., Vaglieco, B.M. (2016). Analysis of combustion of methane and hydrogen–methane blends in small DI SI (direct injection spark ignition) engine using advanced diagnostics. Energy, 108: 99-107. https://doi.org/10.1016/j.energy.2015.09.012
[44] Wang, L., Li, H., Huang, Z., Wang, L., Chen, W. (2023). Impact of hydrogen direct injection on engine combustion and emissions in a GDI engine. Advances in Mechanical Engineering, 15(9): 16878132231189117. https://doi.org/10.1177/16878132231189117
[45] Guardiola, C., Olmeda, P., Pla, B., Bares, P. (2017). In-cylinder pressure based model for exhaust temperature estimation in internal combustion engines. Applied Thermal Engineering, 115: 212-220. https://doi.org/10.1016/j.applthermaleng.2016.12.092
[46] Taymarov, M.A., Akhmetova, R.V., Chiklyayev, Y.G., Lavirko, Y.V., Akhmetov, E.A., Garifullina, A.O. (2019). Study of the speed of flame distribution in the combustion of methane-hydrogen fractions. E3S Web of Conferences, 124: 05065. https://doi.org/10.1051/e3sconf/201912405065
[47] Heywood, J.B. (2018). Internal Combustion Engine Fundamentals. McGraw-Hill Education.
[48] Brunt, M.F., Platts, K.C. (1999). Calculation of heat release in direct injection diesel engines. SAE Transactions, 108: 161-175. https://doi.org/10.4271/1999-01-0187
[49] Krieger, R.B. (1966). The computation of apparent heat release for internal combustion engines. ASME Paper 66-WA/DGP-4.
[50] Gatowski, J.A., Balles, E.N., Chun, K.M., Nelson, F.E., Ekchian, J.A., Heywood, J.B. (1984). Heat release analysis of engine pressure data. SAE Transactions, 93: 961-977. https://doi.org/10.4271/841359
[51] Cheung, H.M., Heywood, J.B. (1993). Evaluation of a one-zone burn-rate analysis procedure using production SI engine pressure data. SAE Transactions, 102: 2292-2303. https://doi.org/10.4271/932749
[52] Eriksson, L., Andersson, I. (2002). An analytic model for cylinder pressure in a four stroke SI engine. SAE Transactions, 111: 726-733. https://doi.org/10.4271/2002-01-0371
[53] Varma, P.S., Mittal, M. (2025). Experimental and numerical investigations to study the effects of hydrogen enrichment on a retrofitted CNG SI engine operating at a low load condition. Fuel, 392: 134914. https://doi.org/10.1016/j.fuel.2025.134914
[54] Farhan, M., Chen, T., Rao, A., Shahid, M.I., Liu, Y., Ma, F. (2024). Comparative knock analysis of HCNG fueled spark ignition engine using different heat transfer models and prediction of knock intensity by artificial neural network fitting tool. Energy, 304: 132135. https://doi.org/10.1016/j.energy.2024.132135
[55] Saleh, F.A., Mahmood, A.S., Allawi, M.K., Al-Sayyab, A.K.S. (2025). The effect of hydrogen on performance of internal combustion engine fueled by compressed natural gas. Journal of Engineering and Sustainable Development, 29(3): 338-343. https://doi.org/10.31272/jeasd.2689
[56] Chterev, I., Boxx, I. (2021). Effect of hydrogen enrichment on the dynamics of a lean technically premixed elevated pressure flame. Combustion and Flame, 225: 149-159. https://doi.org/10.1016/j.combustflame.2020.10.033
[57] Zhang, M., Chang, M., Wang, J., Huang, Z. (2020). Flame dynamics analysis of highly hydrogen-enrichment premixed turbulent combustion. International Journal of Hydrogen Energy, 45(1): 1072-1083. https://doi.org/10.1016/j.ijhydene.2019.10.194
[58] Verhelst, S., Wallner, T. (2009). Hydrogen-fueled internal combustion engines. Progress in Energy and Combustion Science, 35(6): 490-527. https://doi.org/10.1016/j.pecs.2009.08.001

NOMENCLATURE

18HCNG	18% Hydrogen in CNG by volume
25HCNG	25% Hydrogen in CNG by volume
30HCNG	30% Hydrogen in CNG by volume
AFR	Air-Fuel Ratio
BMEP	Brake Mean Effective Pressure
BSFC	Brake Specific Fuel Consumption
CA	Crank Angle, deg
CH_4	Methane
CNG	Compressed Natural Gas
CO	Carbon Monoxide
CO_2	Carbon Dioxide Emissions
GHG	Green House Gas
HC	Hydrocarbon Emissions
HCNG	Hydrogen-enriched Compressed Natural Gas
HRR	Heat Release Rate
HSDA	High Speed Data Acquisition
MBF50	Mass Burn Fraction at 50%
NOx	Nitrogen Oxide Emissions
Pmax	Maximum/Peak Cylinder Pressure, bar
RoPR	Rate of Pressure Rise
RPM	Revolutions Per Minute
SI	Spark Ignition
TDC	Top Dead Center
UHC	Unburned Hydrocarbons

Greek symbols

λ	Lambda
κ	Variable Polytropic Exponent